# Essentials of Recrystallization

Sylvia Dickey

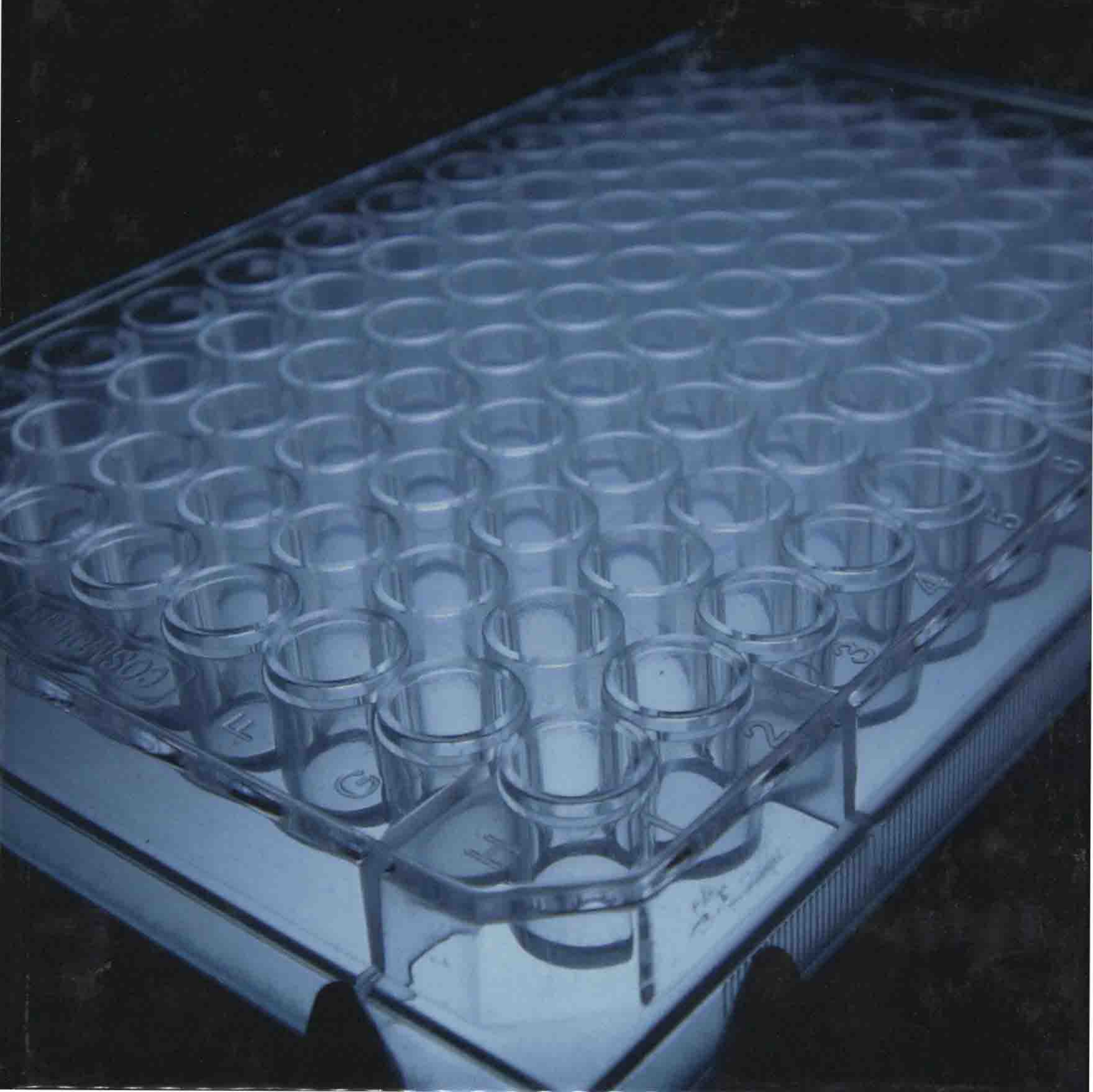

# Essentials of Recrystallization

Edited by **Sylvia Dickey**

NY RESEARCH PRESS
New York

Published by NY Research Press,
23 West, 55th Street, Suite 816,
New York, NY 10019, USA
www.nyresearchpress.com

**Essentials of Recrystallization**
Edited by Sylvia Dickey



International Standard Book Number: 978-1-63238-193-4 (Hardback)



Printed in China.

# Essentials of Recrystallization

# Preface

Recrystallization is a substantial process in geology and metallurgical science. This book discusses recent researches and techniques introduced in various fields where recrystallization is considered as an essential process. With the advancements in technologies like TEM, spectrometers, etc., it is becoming convenient to produce better and accurate results. This book sheds light on approaches like improving properties of alloys, using new sophisticated devices to image grains and studying the problems of recrystallization in frozen aqueous solutions. This book will be helpful for scientists and students interested in learning more about recrystallization.

All of the data presented henceforth, was collaborated in the wake of recent advancements in the field. The aim of this book is to present the diversified developments from across the globe in a comprehensible manner. The opinions expressed in each chapter belong solely to the contributing authors. Their interpretations of the topics are the integral part of this book, which I have carefully compiled for a better understanding of the readers.

At the end, I would like to thank all those who dedicated their time and efforts for the successful completion of this book. I also wish to convey my gratitude towards my friends and family who supported me at every step.

**Editor**

# Contents

Section 1

# General Topics in Recrystallization

Chapter 1

# Recrystallization Textures of Metals and Alloys

Dong Nyung Lee and Heung Nam Han

Additional information is available at the end of the chapter

## 1. Introduction

Recrystallization (Rex) takes place through nucleation and growth. Nucleation during Rex can be defined as the formation of strain-free crystals, in a high energy matrix, that are able to grow under energy release by a movement of high-angle grain boundaries. The nucleus is in a thermodynamic equilibrium between energy released by the growth of the nucleus (given by the energy difference between deformed and recrystallized volume) and energy consumed by the increase in high angle grain boundary area. This means that a critical nucleus size or a critical grain boundary curvature exists, from which the newly formed crystal grows under energy release. This definition is so broad and obscure that crystallization of amorphous materials is called Rex by some people, and Rex can be confused with the abnormal grain growth when grains with minor texture components can grow at the expense of neighboring grains with main texture components because the minor-component grains can be taken as nuclei. Here we will present a theory which can determine whether grains survived during deformation act as nuclei and which orientation the deformed matrix is destined to assume after Rex. A lot of Rex textures will be explained by the theory.

## 2. Theories for evolution of recrystallization textures

Rex occurs by nucleation and growth. Therefore, the evolution of the Rex texture must be controlled by nucleation and growth. In the oriented nucleation theory (ON), the preferred activation of a special nucleus determines the final Rex texture [1]. In the oriented growth theory (OG), the only grains having a special relationship to the deformed matrix can preferably grow [2]. Recent computer simulation studies tend to advocate ON theory [3]. This comes from the presumption that the growth of nuclei is predominated by a difference in energy between the nucleus and the matrix, or the driving force. In addition to this, the weakness of the conventional OG theory is in much reliance on the grain boundary mobility.

One of the present authors (Lee) advanced a theory for the evolution of Rex textures [4] and elaborated later [5,6]. In the theory, the Rex texture is determined such that the absolute maximum stress direction (AMSD) due to dislocation array formed during fabrication and subsequent recovery is parallel to the minimum Young's modulus direction (MYMD) in recrystallized (Rexed) grains and other conditions are met, whereby the strain energy release can be maximized. In the strain-energy-release-maximization theory (SERM), elastic anisotropy is importantly taken into account.

In what follows, SERM is briefly described. Rex occurs to reduce the energy stored during fabrication by a nucleation and growth process. The stored energy may include energies due to vacancies, dislocations, grain boundaries, surface, etc. The energy is not directional, but the texture is directional. No matter how high the energy may be, the defects cannot directly be related to the Rex texture, unless they give rise to some anisotropic characteristics. An effect of anisotropy of free surface energy due to differences in lattice surface energies can be neglected except in the case where the grain size is larger than the specimen thickness in vacuum or an inert atmosphere. Differences in the mobility and/or energy of grain boundaries must be important factors to consider in the texture change during grain growth. Vacancies do not seem to have an important effect on the Rex texture due to their relatively isotropic characteristics. The most important driving force for Rex (nucleation and growth) is known to be the stored energy due to dislocations. The dislocation density may be different from grain to grain. Even in a grain the dislocation density is not homogeneous. Grains with low dislocation densities can grow at the expanse of grains with high dislocation densities. This may be true for slightly deformed metals as in case of strain annealing. However, the differences in dislocation density and orientation between grains decrease with increasing deformation. Considering the fact that strong deformation textures give rise to strong Rex textures, the dislocation density difference cannot be a dominant factor for the evolution of Rex textures. Dislocations cannot be related to the Rex texture, unless they give rise to anisotropic characteristics.

The dislocation array in fabricated materials looks very complicated. Dislocations generated during plastic deformation, deposition, etc., can be of edge, screw, and mixed types. Their Burgers vectors can be determined by deformation mode and texture, and their array can be approximated by a stable or low energy arrangement of edge dislocations after recovery. Figure 1 shows a schematic dislocation array after recovery and principal stress distributions around stable and low energy configurations of edge dislocations, which were calculated using superposition of the stress fields around isolated dislocations, or, more specifically, were obtained by a summation of the components of stress field of the individual dislocations sited in the array. It can be seen that AMSD is along the Burgers vector of dislocations that are responsible for the long-range stress field. The volume of crystal changes little after heavy deformation because contraction in the compressive field and expansion in the tensile fields around dislocations generated during deformation compensate each other. That is, this process takes place in a displacement controlled system. The uniaxial specimen in Figure 2 makes an example of the displacement controlled system. When a stress-free specimen $S_0$ is elastically elongated by $\Delta L$ by force $F_A$ (Figure 2a), the elongated specimen $S_F$ has an elastic strain energy represented by triangle *OAC* (Figure 2b). When V in $S_F$ is replaced by a stress-free volume V, $S_R$ having the stress free V has the strain energy of *OBC* (Figure 2b. ) Transformation from the $S_F$ state to the $S_R$ state results in a strain-energy-release represented by *OAB* (Figure 2b). The strain-energy-release can be maximized when the $S_F$ and $S_R$ states have the maximum and minimum strain energies, respectively. In this case, AMSD is the axial direction of $S_F$, and the $S_R$ state has the minimum energy when MYMD of the stress-free V is along the axial direction that is AMSD. In summary, the strain energy release is maximized when AMSD in the high dislocation density matrix is along MYMD of the stress free crystal, or nucleus. That is, when a volume of *V* in the stress field is replaced by a stress-free single crystal of the volume *V*, the strain energy release of the system occurs. The strain energy release can change depending on the orientation of the stress-free crystal. The strain energy release is maximized when AMSD in the high energy matrix is along MYMD of the stress-free crystal. The stress-free grains formed in the early stage are referred to as nuclei, if they can grow. The orientation of a nucleus is determined such that its strain energy release per unit volume during Rex becomes maximized.

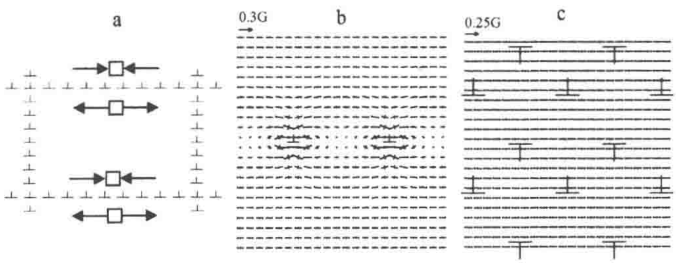


**Figure 1.** (a) Schematic dislocation array after recovery, where horizontal arrays give rise to long-range stress field, and vertical arrays give rise to short-range stress field [7]. Principal stress distributions around parallel edge dislocations calculated based on (b) 100 linearly arrayed dislocations with dislocation spacing of 10**b**, and (c) low energy array of 100 x 100 dislocations. **b** is Burgers vector and G is shear modulus [8].

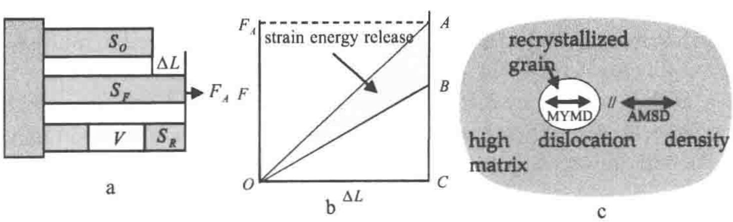


**Figure 2.** Displacement controlled uniaxial specimen for explaining strain-energy-release being maximized when AMSD in high dislocation density matrix is along MYMD in recrystallized grain.

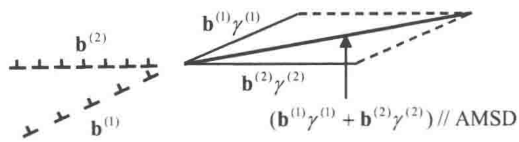


**Figure 3.** AMSD for active slip systems $i$ whose Burgers vectors are $\mathbf{b}^{(i)}$ and activities are $\gamma^{(i)}$.

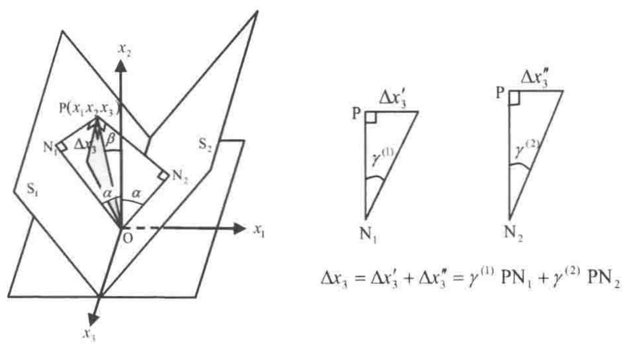


**Figure 4.** Schematic of two slip planes $S_1$ and $S_2$ that share common slip direction along $x_3$ axis.

We first calculate AMSD in an fcc crystal deformed by a duplex slip of (111)[-101] and (111)[-110] that are equally active. The duplex slip can be taken as a single slip of (111)[-211], which is obtained by the sum of the two slip directions. In this case, the maximum stress direction is [-211]. However, some complication can occur. One slip system has two opposite directions. The maximum stress direction for the (111)[-101] slip system represents the [-101] direction and its opposite direction, [1 0-1]. The maximum stress direction for the (111)[-110] slip system represents the [-110] and [1-1 0] directions. Therefore, there are four possible combinations to calculate the maximum stress direction, [-101] + [-110] = [-211], [-101] + [1-1 0] = [0-1 1], [1 0-1] + [-110] = [0 1-1], and [1 0-1] + [1-1 0] = [2-1-1], among which [-211]//[2-1-1] and [0-1 1]//[0 1-1]. The correct combinations are such that two directions make an acute angle. If the two slip systems are not equally active, the activity of each slip system should be taken into account. If the (111)[-101] slip system is two times more active than the (111)[-110] system, the maximum stress direction becomes 2[-101] + [-110] = [-312]. This can be generalized to multiple slip. For multiple slip, AMSD is calculated by the sum of active slip directions of the same sense and their activities, as shown in Figure 3. It is convenient to choose slip directions so that they can be at acute angles with the highest strain direction of the specimen, e.g., RD in rolled sheets, the axial direction in drawn wires, etc.

When two slip systems share the same slip direction, their contributions to AMSD are reduced by 0.5 for bcc metals and 0.577 for fcc metals as follows. Figure 4 shows two slip planes, $S_1$ and $S_2$, intersecting along the common slip direction, the $x_3$ axis; the $x_2$ axis bisects the angle between the poles of these planes. The loading direction lies within the quadrant drawn between $S_1$ and

$S_2$, and the displacement $\Delta x_3$ along the $x_3$ axis at any point P with coordinates $(x_1, x_2, x_3)$ is considered. If shear strains $\gamma^{(1)}$ and $\gamma^{(2)}$ occur on the slip system 1 (the slip plane $S_1$ and the slip direction $x_3$) and the slip system 2 (the slip plane $S_2$ and the slip direction $x_3$), respectively, then

$$\Delta x_3 = \gamma^{(1)}\ \mathrm{PN}_1 + \gamma^{(2)}\ \mathrm{PN}_2 \tag{1}$$

where $\mathrm{PN}_1$ and $\mathrm{PN}_2$ are normal to the planes $S_1$ and $S_2$, respectively. Therefore,

$$\mathrm{PN}_1 = \mathrm{OP}\ \sin(\alpha - \beta) \text{and}\ \ \mathrm{PN}_2 = \mathrm{OP}\ \sin(\alpha + \beta) \tag{2}$$

where OP, $\alpha$, and $\beta$ are defined in Figure 4. Therefore,

$$\Delta x_3 = (\gamma^{(1)} + \gamma^{(2)})\ \mathrm{OP}\ \sin\alpha\cos\beta + (\gamma^{(2)} - \gamma^{(1)})\ \mathrm{OP}\ \cos\alpha\sin\beta \tag{3}$$

Because $\alpha > \beta$ and $(\gamma^{(1)} + \gamma^{(2)}) > (\gamma^{(2)} - \gamma^{(1)})$, the second term of the right hand side is negligible compared with the first term. It follows from OP $\cos\beta = x_2$ that $\Delta x_3 \approx (\gamma^{(1)} + \gamma^{(2)})\, x_2 \sin\alpha$. Therefore, the displacement $\Delta x_3$ is linear with the $x_2$ coordinate, and the deformation is equivalent to single slip in the $x_3$ direction on the $(\gamma^{(1)}S_1 + \gamma^{(2)}S_2)$ plane. The apparent shear strain $\gamma_a$ is

$$\gamma_a = \Delta x_3 / x_2 \approx (\gamma^{(1)} + \gamma^{(2)})\ \sin\alpha \tag{4}$$

The apparent shear strains $\gamma_a^{(i)}$ on the slip systems $i$ are

$$\gamma_a^{(i)} = \gamma^{(i)} \sin\alpha \tag{5}$$

For bcc metals, $\sin\alpha = 0.5$ (e.g. a duplex slip of (101)[1 1-1] and (011)[1 1-1]) and hence

$$\gamma_a^{(i)}(\mathrm{bcc}) = 0.5\gamma^{(i)} \tag{6}$$

For fcc metals, $\sin\alpha = 0.577$ (e.g. a duplex slip of (-1 1-1)[110] and (1-1-1)[110]) and hence

$$\gamma_a^{(i)}(\mathrm{fcc}) = 0.577\gamma^{(i)} \tag{7}$$

The activity of each slip direction is linearly proportional to the dislocation density $\rho$ on the corresponding slip system, which is roughly proportional to the shear strain on the slip system. Experimental results on the relation between shear strain $\gamma$ and $\rho$ are available for Cu and Al [9].

If a crystal is plastically deformed by $\delta\varepsilon$ (often about 0.01), then we can calculate active slip systems $i$ and shear strains $\gamma^{(i)}$ on them using a crystal plasticity model, resulting in the shear strain rate with respect to strain of specimen, $d\gamma^{(i)}/d\varepsilon$. During this deformation, the crystal can rotate, and active slip systems and shear strains on them change during $\delta\varepsilon$. When a crystal rotates during deformation, the absolute value of shear strain rates $|d\gamma^{(i)}/d\varepsilon|$ on slip systems $i$ can vary with strain $\varepsilon$ of specimen. For a strain up to $\varepsilon = e$, the contribution of each slip system to AMSD is proportional to

$$\gamma^{(i)} = \int_0^e \left| d\gamma^{(i)} / d\varepsilon \right| d\varepsilon \tag{8}$$

The above equation is illustrated in Figure 5. If a deformation texture is stable, the shear strain rates on the slip systems are independent of deformation.

So far methods of obtaining AMSD have been discussed. This is good enough for prediction of fiber textures. However, the stress states around dislocation arrays are not uniaxial but triaxial. Unfortunately we do not know the stress fields of individual dislocations in real crystals, but know Burgers vectors. Therefore, AMSD obtained above applies to real crystals. Any stress state has three principal stresses and hence three principal stress directions which are perpendicular to each other. Once we know the three principal stress directions, the Rex textures are determined such that the three directions in the deformed matrix are parallel to three <100> directions in the Rexed grain, when MYMDs are <100>. In figure 6, let the unit vectors of **A**, **B**, and **C** be $\boldsymbol{a}$ $[a_1\ a_2\ a_3]$, $\boldsymbol{b}$ $[b_1\ b_2\ b_3]$, and $\boldsymbol{c}$ $[c_1\ c_2\ c_3]$, where $a_i$ are direction cosines of the unit vector $\boldsymbol{a}$ referred to the crystal coordinate system. AMSD is one of three principal stress directions. Two other principal stresses are obtained as explained in Figure 6.

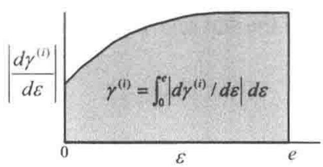


**Figure 5.** Calculation of $\gamma^{(i)}$ for crystal rotation during deformation up to $\varepsilon = e$.

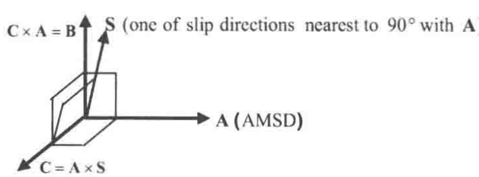


**Figure 6.** Relationship between three principal stress directions **A**, **B**, and **C**.

If the unit vectors $\boldsymbol{a}$, $\boldsymbol{b}$, and $\boldsymbol{c}$ are set to be along [100], [010], and [001] after Rex, components of the unit vectors are direction cosines relating the deformed and Rexed crystal coordinate systems, when MYMDs are <100>. That is, the $(hkl)[uvw]$ deformation orientation is calculated to transform to the $(h_r\ k_r\ l_r)[u_r\ v_r\ w_r]$ Rex orientation using the following equation.